

Novel electron-type host material for unilateral homogeneous phosphorescent organic light-emitting diodes with low efficiency roll-off†

Xiao Yang,^a Hong Huang,^a Biao Pan,^a Shaoqing Zhuang,^a Matthew P. Aldred,^a Lei Wang,^{*a} Jiangshan Chen^{*b} and Dongge Ma^b

Received 20th June 2012, Accepted 16th September 2012

DOI: 10.1039/c2jm33988a

Two novel simple electron-transport (ET) type host materials, 2,6-bis(3-(1-phenyl-1*H*-benzo[d]imidazol-2-yl)phenyl)benzene (**MDBIP**) and 2,6-bis(3-(1-phenyl-1*H*-benzo[d]imidazol-2-yl)phenyl)pyridine (**MDBIPy**) have been designed and synthesized. The two compounds exhibit high decomposition temperatures (T_d : 444 °C for **MDBIP** and 450 °C for **MDBIPy**) and a stable amorphous glassy state (T_g : 108 °C for **MDBIP** and 110 °C for **MDBIPy**). In the typical device ITO/MoO₃ (10 nm)/4,4'-bis[*N*-(1-naphthyl)-*N*-phenylamino]biphenyl (NPB, 80 nm)/TCTA (5 nm)/Host: Ir(ppy)₃ (9 wt%, 20 nm)/TmPyPB (40 nm)/LiF (1 nm)/Al (100 nm), when **MDBIP** was used as host material, the device B showed a maximum efficiency of 21.1%, 75.8 cd A⁻¹ and 83.6 lm W⁻¹. When **MDBIPy** was utilized as both the electron transporting and host layer, the unilateral homogeneous device C exhibited a maximum efficiency of 20.6%, 74.2 cd A⁻¹ and 71.8 lm W⁻¹. More interestingly, device C showed low efficiency roll-off relative to device B. When the brightness of the device is over 1000 cd m⁻², the current efficiency of device C is higher than device B. At a brightness of 5000 cd m⁻², the current efficiency of device C is only roll off 5.6%. These results demonstrate that utilizing electron-transport type host materials to fabricate unilateral homogeneous PhOLEDs is a promising way to simplify the device configuration and optimize the performance of OLED devices.

1. Introduction

Phosphorescent organic light-emitting diodes (PhOLEDs) have attracted much attention because they can achieve 100% internal quantum efficiency by incorporating triplet and singlet emitters.¹ Owing to these, PhOLEDs are the most noticeable candidates for full-color flat-panel displays and solid-state lighting.² For the purpose of obtaining highly efficient PhOLEDs, the selection of a suitable host material for the phosphorescent dopant is important. A suitable host–dopant system could fundamentally affect the device efficiency and the energy transfer from the host to the dopant. In general, in order to achieve efficient electrophosphorescence, the following principles for the host material should be followed: firstly, the triplet energy (E_T) of the host materials must be higher than that of the dopants. Secondly, the host materials should have good charge-carrier transport properties, which can increase the recombination opportunities for

electrons and holes, and decrease the drive voltage and improve the device efficiency.³ Finally, the highest occupied molecular orbital (HOMO)/lowest unoccupied molecular orbital (LUMO) level should be matched with the adjacent layer, which will reduce the interface energy barrier, and reduce the efficiency roll-off, which arises from triplet–triplet annihilation (TTA) or triplet exciton–polaron quenching (TPQ) at high current densities.⁴

In order to balance the electron–hole carriers, broaden the recombination zone and reduce the efficiency roll-off at high brightness, more researchers have turned their attention to the development of bipolar host materials.⁵ For example, Chou and Cheng designed and synthesized a green host material BCPO for iridium(III) fac-tris(2-phenylpyridine) (Ir(ppy)₃), which showed a relatively low turn-on voltage of 2.1 V and a maximum external quantum efficiency (EQE) of 21.6%.⁶ Kido *et al.* developed a new bipolar host material based on carbazole and pyridine for green OLEDs, which exhibited a maximum EQE and power efficiency of 25.2% and 102 lm W⁻¹, respectively.⁷ Yang *et al.* reported a carbazole/oxadiazole hybrid molecule *o*-CzOXD⁸ for green and red phosphorescent devices. The device exhibits a maximum EQE as high as 20.2% for green and 18.5% for red electrophosphorescence. However, for most host materials, the electron mobility is lower than that of holes, so it is also a very efficient way to design and synthesize ET-type host materials to balance the carriers and improve the device performance.⁹ Chiu *et al.* reported an electron-transport type host OXD based on

^aWuhan National Laboratory for Optoelectronics, School of Optoelectronic Science and Engineering, Huazhong University of Science and Technology, Wuhan 430074, P. R. China. E-mail: wanglei@mail.hust.edu.cn

^bState Key Laboratory of Polymer Physics and Chemistry, Changchun Institute of Applied Chemistry, Graduate School of Chinese Academy of Sciences, Chinese Academy of Sciences, Changchun 130022, P. R. China. E-mail: jschen@ciac.jl.cn

† Electronic supplementary information (ESI) available. See DOI: 10.1039/c2jm33988a

oxadiazole, which showed a maximum current efficiency of 17.2%, when doped with FIrpic.¹⁰ Lee *et al.* designed electron-transport type host materials based on pyridine, which exhibited a high external quantum efficiency of 13.3% in red phosphorescent organic light-emitting diodes.¹¹ Leung *et al.* reported an effective electron transport host BOBP, which exhibits a maximum brightness of 43 000 cd m⁻² with an efficiency of 26 cd A⁻¹ in green phosphorescent organic light-emitting diodes.¹² However, as we know, the procedure for fabricating these devices is complex and the device performances still need further improvement. ET-type materials, serving as the host layer and electron transport layer (ETL) simultaneously, can be used to construct simple unilateral homogeneous phosphorescent OLED, which will reduce the interface energy barrier between EML and ETL, broaden the exciton recombination zone and improve the device performances. Wong *et al.* synthesized a new ET-type host based on 1,3,5-triazine derivatives, 2,4,6-tris(biphenyl-3-yl)-1,3,5-triazine (T2T), and in a unilateral homogeneous device, the maximum efficiencies reached up to 15.7%, 54 cd A⁻¹, 56 lm W⁻¹, respectively.¹³ Takizawa *et al.* fabricated a green unilateral homogeneous device with TPBI as the host material and ETL, but the maximum efficiencies are only 5.7%, 26.4 cd A⁻¹, 33.2 lm W⁻¹.¹⁴ Therefore, it is still a great challenge to design new ET-type host materials that can be used as the host layer and ET layer, simultaneously.

In this paper, we report two new ET type host materials, **MDBIP** and **MDBIPy**, based on benzimidazole, in which the electron affinity and HOMO/LUMO were modified by introducing different linking spacers, such as benzene and pyridine, respectively. The HOMO/LUMO orbitals of the compound **MDBIPy** are almost completely separate and exhibit high electron mobility. When **MDBIPy** was used as the host material for the doped emitter material Ir(ppy)₃, the device B exhibited maximum external quantum/current/power efficiencies of 21.1%, 75.8 cd A⁻¹ and 83.6 lm W⁻¹, respectively. Meanwhile, the device C with **MDBIPy** as ETL and host showed a maximum EQE, current efficiency and power efficiency of 20.6%, 74.2 cd A⁻¹ and 71.8 lm W⁻¹, respectively. More interestingly, the current efficiency of device C at a brightness of 1000 and 5000 cd m⁻² exhibits efficiency roll-off of only 1.1% and 5.6%, respectively.

2. Experimental section

2.1. General information

All solvents and materials were used as received from commercial suppliers without further purification. The synthetic routes of the **MDBIP** and **MDBIPy** are outlined in Scheme 1. ¹H NMR and ¹³C NMR spectra were measured on a Bruker-AF301 AT 400 MHz spectrometer. Elemental analyses of carbon, hydrogen, and nitrogen were performed on an Elementar (Vario Micro cube) analyzer. Mass spectra were carried out on an Agilent (1100 LC/MSD Trap) using ACPI ionization. UV-Vis absorption spectra were recorded on a Shimadzu UV-VIS-NIR spectrophotometer (UV-3600). PL spectra were recorded on Edinburgh instruments (FLSP920 spectrometers). Differential scanning calorimetry (DSC) was performed on a PE Instruments DSC 2920 unit at a heating rate of 10 °C min⁻¹ from 30 to 250 °C under nitrogen.

The glass transition temperature (T_g) was determined from the second heating scan. Thermogravimetric analysis (TGA) was undertaken with a PerkinElmer Instruments (Pyris1 TGA). The thermal stability of the samples under a nitrogen atmosphere was determined by measuring their weight loss while heating at a rate of 10 °C min⁻¹ from 30 to 700 °C. Cyclic voltammetry measurements were carried out in a conventional three electrode cell using a Pt button working electrode of 2 mm in diameter, a platinum wire counter electrode, and an Ag/AgNO₃ (0.1 M) reference electrode on a computer-controlled EG&G Potentiostat/Galvanostat model 283 at room temperature. Reduction CVs of all compounds were performed in dichloromethane containing 0.1 M tetrabutylammoniumhexafluorophosphate (Bu₄NPF₆) as the supporting electrolyte. The onset potential was determined from the intersection of two tangents drawn at the rising and background current of the cyclic voltammogram.

2.2. Computational details

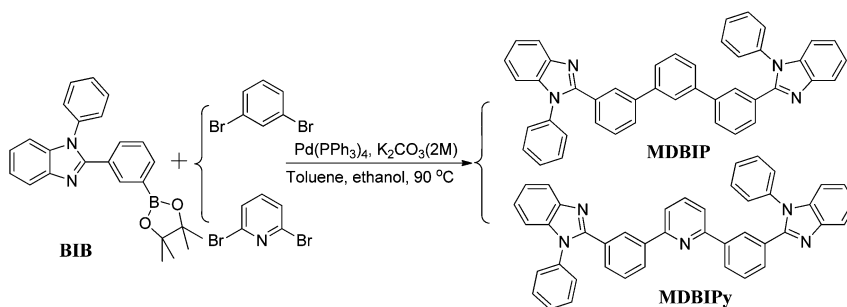
The geometrical and electronic properties were performed with the Amsterdam Density Functional (ADF) 2009.01 program package. The calculation was optimized by means of the B3LYP (Becke three parameters hybrid functional with Lee–Yang–Perdew correlation functionals)¹⁵ with the 6-31 G(d) atomic basis set. Then the electronic structures were calculated at τ -HCTHhyb/6-311++G(d, p) level.¹⁶ Molecular orbitals were visualized using ADFview.

2.3. Device fabrication and measurement

The EL devices were fabricated by vacuum deposition of the materials at a base pressure of 5×10^{-6} Torr onto glass pre-coated with a layer of indium tin oxide (ITO) with a sheet resistance of 20 Ω per square. Before deposition of an organic layer, the clear ITO substrates were treated with oxygen plasma for 5 min. The deposition rate of organic compounds was 0.9–1.1 Å s⁻¹. Finally, a cathode composed of LiF (1 nm) and aluminum (100 nm) was sequentially deposited onto the substrate in the vacuum of 10^{-5} Torr. The L - V - J of the devices was measured with a Keithley 2400 Source meter and PR655. All measurements were carried out at room temperature under ambient conditions.

2.4. Synthesis

Compound 3,3''-bis(1-phenyl-1*H*-benzo[d]imidazol-2-yl)-1,1':3',1''-terphenyl (MDBIP). A mixture of the compound 1-phenyl-2-(3-(4,4,5,5-tetramethyl-1,3,2-dioxaborolan-2-yl)phenyl)-1*H*-benzo[d]imidazole (2.2 mmol), 1,3-dibromobenzene (1.0 mmol), Pd(PPh₃)₄ (0.05 mmol), K₂CO₃ (2.0 M aqueous solution) (25 ml), toluene (50 ml) and ethanol (25 ml) was stirred at 90 °C for 24 h. After it was cooled to room temperature, the dichloromethane was added to the reaction mixture. The organic phase was separated and washed with brine before drying over anhydrous MgSO₄. The solvent was evaporated off, and the solid residues were purified by column chromatography on silica gel with petroleum ether to afford the final compound as a white solid. Yield: 80%. ¹H NMR (400 MHz, CDCl₃) δ (ppm): 7.93–7.92 (d, J = 8.0 Hz, 2H), 7.76 (s, 2H), 7.68–7.66 (d, J = 7.6 Hz, 2H), 7.58–7.52 (m, 6H), 7.47–7.44 (m, 4H), 7.42–7.34 (m, 7H), 7.33–7.27 (m, 7H). ¹³C NMR (100 MHz, CDCl₃) δ (ppm): 152.16, 140.96,



Scheme 1 The synthetic routes toward the bipolar hosts **MDBIP** and **MDBIPy**.

140.92, 137.29, 137.16, 130.37, 130.03, 129.11, 128.81, 128.77, 128.53, 128.41, 127.59, 126.31, 125.88, 123.50, 123.11, 119.93, 119.90, 110.51. MS (APCI): calcd for $C_{44}H_{30}N_4$: 614.2, found, 615.4 ($M+1$)⁺. Anal. calcd. C, 85.97, H, 4.92, N, 9.11, found C, 85.94, H, 4.85, N, 9.15%.

Compound 2,6-bis(3-(1-phenyl-1H-benzo[d]imidazol-2-yl)phenyl)pyridine (MDBIPy). The compound **MDBIPy** was prepared according to the same procedure as the compound **MDBIP** but using 2,6-dibromopyridine to instead 1,3-dibromobenzene. Yield: 84%. ¹H NMR (400 MHz, $CDCl_3$) δ (ppm): 8.28–8.27 (m, 2H), 8.15–8.13 (d, $J = 8.0$ Hz, 2H), 7.94–7.92 (d, $J = 8.0$ Hz, 2H), 7.94–7.92 (m, 1H), 7.72–7.70 (d, $J = 8.0$ Hz, 2H), 7.52–7.42 (m, 10H), 7.39–7.28 (m, 10H). ¹³C NMR (100 MHz, $CDCl_3$) δ (ppm): 155.95, 152.27, 142.98, 139.43, 137.50, 137.26, 137.07, 130.26, 129.99, 129.95, 128.75, 128.61, 128.26, 128.05, 127.52, 123.48, 123.11, 119.90, 118.93, 110.54. MS (APCI): calcd for $C_{43}H_{29}N_5$: 615.2, found, 616.4 ($M+1$)⁺. Anal. calcd. C, 83.88, H, 4.75, N, 11.37, found C, 83.68, H, 4.72, N, 11.42%.

3. Results and discussion

3.1. Synthesis and characterization

Scheme 1 illustrates the synthetic routes for the target molecules. The key intermediate benzimidazole boronic ester (**BIB**) was synthesized according to the literature.¹⁷ The target host materials **MDBIP** and **MDBIPy** were readily synthesized by the typical Suzuki coupling reaction of **BIB** with 1,3-dibromobenzene or 2,5-dibromopyridine in high yield (>80%). All the target materials were further purified by repeated temperature-gradient vacuum sublimation before testing. The two target compounds were fully characterized by ¹H NMR and ¹³C NMR spectroscopies, mass spectrometry and elemental analysis.

3.2. Thermal properties and morphological properties

The thermal properties of compounds **MDBIP** and **MDBIPy** were determined by thermogravimetric analysis (TGA) and differential scanning calorimetry (DSC) (Fig. 1). Because the two compounds have similar chemical structures and molecular weights, they also show similar thermal properties. The detailed thermal data of these compounds are listed in Table 1. The compounds **MDBIP** and **MDBIPy** exhibit relatively high glass transition temperatures (T_g) of 108 °C, and 110 °C in the DSC

heating cycle, respectively, which are significantly higher than the T_g of widely used 4,4-*N,N'*-carbazole-biphenyl (CBP: 62 °C).¹⁸ In addition, the compounds **MDBIP** and **MDBIPy** also exhibit good thermal stability with decomposition temperatures (T_d , 5% weight loss) at 444 and 450 °C for **MDBIP** and **MDBIPy**, respectively. The relatively high T_g and T_d values make these compounds avoid phase separation upon heating and they have the potential for fabrication into high performance devices by vacuum thermal evaporation technology.

Since efficient film-forming properties of light emitting materials are crucial for the performance of devices, the surface morphologies of vacuum-deposited thin films of **MDBIP** and **MDBIPy** were studied by atomic force microscopy (AFM). As shown in Fig. 2, the solid film samples exhibit a root-mean-square (RMS) roughness of 0.647 and 0.369 nm for **MDBIP** and **MDBIPy**, respectively. The relatively small RMS of **MDBIPy** in the thin films makes it desirable for high performance OLEDs.

3.3. Photophysical properties

Fig. 3(a) shows the UV-Vis absorption and photoluminescence spectra of **MDBIP** and **MDBIPy** in dilute toluene solution. The two compounds exhibit similar absorption. The maximum absorption at around 292 nm may be attributed to the π - π^* transition from benzimidazole. The maximum PL emission peaks of **MDBIP** and **MDBIPy** are 352 nm and 351 nm, respectively. The two compounds show similar absorption and emission spectra which can be ascribed to their similar spatial structure. The phosphorescence spectra of **MDBIP** and **MDBIPy** in 2-methyltetrahydrofuran solution at 77 K show the highest energy peaks at 478 and 484 nm, respectively (Fig. 3(b)), which correspond to triplet energy levels at 2.60 and 2.56 eV. Generally, green phosphorescent emitters such as Ir(ppy)₃ possess triplet energy levels at about 2.43 eV, indicating that both **MDBIP** and **MDBIPy** can act as appropriate host materials for green phosphorescent emitters.

3.4. Electrochemical properties

Cyclic voltammetry (CV) was performed to investigate the electrochemical properties of **MDBIP** and **MDBIPy** (Fig. 4). The compounds exhibit irreversible oxidation due to the instability of their radical cations.¹⁹ HOMO and LUMO energy levels of the two compounds were calculated from the onset potentials for oxidation together with their absorption spectra (Table 1). The

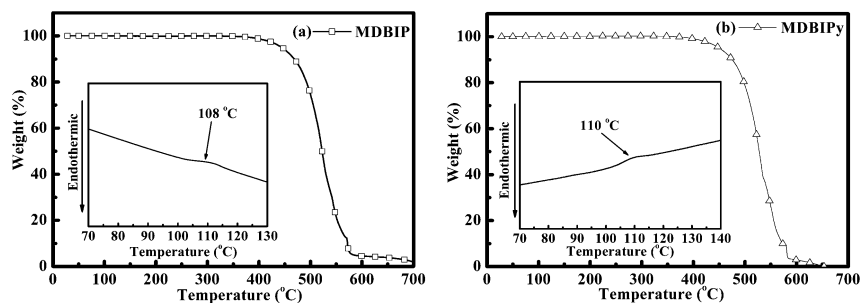


Fig. 1 The TGA thermograms of the compounds **MDBIP** (left) and **MDBIPy** (right) recorded at a heating rate of $10\text{ }^{\circ}\text{C min}^{-1}$. Inset: the DSC traces of the compounds **MDBIP** and **MDBIPy** recorded at a heating rate of $10\text{ }^{\circ}\text{C min}^{-1}$.

HOMO/LUMO levels of the **MDBIP** and **MDBIPy** are 5.90/2.36 and 5.89/2.19 eV, respectively. This can reduce the hole injection barrier from the hole transporting layer (HTL) to **MDBIP** and **MDBIPy**, compared with commercial host materials such as TPBI (6.3 eV).²⁰

3.5. Theoretical calculations

To understand the electronic structures of **MDBIP** and **MDBIPy**, density functional theory (DFT) calculations were performed at a B3LYP/6-31 G(d) level for the geometry optimization. As shown in Fig. 5, both the HOMO and LUMO orbitals of **MDBIP** are mainly dispersed on the benzimidazole units, whereas for the compound **MDBIPy**, the LUMO is dispersed on the benzimidazole, and the HOMO is located on the linking spacer 2,6-diphenylpyridine. Since separation between the HOMO and LUMO levels is preferable for the prevention of reverse energy transfer,^{17,21} **MDBIPy** may be more suitable as a host material for Ir(ppy)₃ as compared with **MDBIP**. The calculated HOMO/LUMO values are 5.65/2.41 for **MDBIP**, and 5.56/2.55 for **MDBIPy**, which correlate well with the observations from cyclic voltammetry (see Table 1). By the way, because of the separation of the HOMO and LUMO, **MDBIPy** may possess intramolecular charge transfer (CT) emission. The PL spectra of **MDBIPy** in THF solution exhibit a longer wavelength PL peak, which also verified these features (see Fig. S1†).

3.6. Electroluminescence

In order to investigate the utility of **MDBIP** and **MDBIPy** as host materials for the green phosphor Ir(ppy)₃, green PhOLEDs with the structure of ITO/MoO₃ (10 nm)/NPB (80 nm)/TCTA (5 nm)/Host: Ir(ppy)₃ (9 wt%, 20 nm)/TmPyPB (40 nm)/LiF (1 nm)/Al (100 nm) were fabricated. The relative HOMO/LUMO energy levels of the materials are illustrated in Fig. 6. MoO₃ and

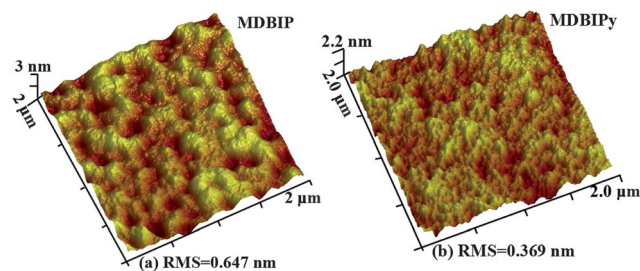


Fig. 2 AFM topographic images of the **MDBIP** and **MDBIPy**.

LiF were employed as the hole injection layer (HIL) and electron injection layer (EIL), respectively. NPB and TmPyPB act as the hole and electron transport layers (HTL/ETL), respectively. A pure thin TCTA layer with a high triplet energy ($E_T = 2.85\text{ eV}$)²² was used as the exciton blocking layer (EBL) to prevent exciton diffusion and improve the efficiency. The green phosphorescent dopant Ir(ppy)₃ was co-evaporated with the host materials to examine the performance of the new electron-type host materials **MDBIP** (device A) and **MDBIPy** (device B).

The current density (J)–voltage (V)–brightness (B) characteristics, and the efficiency curves of devices A and B are shown in Fig. 7(a) and (b), respectively. The EL data of the devices are summarized in Table 2. Both device A and B exhibit low turn-on voltages (2.8 V for device A, 2.7 V for device B), which could be attributed to their matching HOMO levels with TCTA (5.8 eV). As shown in Fig. 7(a), the drive voltage of device A is remarkably higher than device B, such as at a current density of 40 mA cm^{-2} the drive voltages of devices A and B are 9.3 and 7.8 V, respectively. Device B hosted by **MDBIPy** exhibits a maximum EQE of 21.1%, a maximum current efficiency of 75.8 cd A^{-1} and a power efficiency of 83.6 lm W^{-1} , which are significantly higher than those for **MDBIP** (17.8% , 63.7 cd A^{-1} , 65.8 lm W^{-1}). The relatively low drive voltage and high performance of device B compared to device A may be due to the separation of the

Table 1 The photophysical and electrochemical properties of **MDBIP** and **MDBIPy**^a

	Abs (nm)	PL (nm)	E_g (eV)	HOMO/LUMO _{exp} (eV)	HOMO/LUMO _{cal} (eV)	E_T (eV)	T_g/T_d (°C)
MDBIP	292	352	3.71	5.90/2.19	5.65/2.41	2.60	108/444
MDBIPy	292	352	3.68	5.89/2.21	5.56/2.55	2.56	110/450

^a HOMO/LUMO_{exp}: measured from the CV; HOMO/LUMO_{cal}: calculated from the DFT; E_g : calculated from the onset of the absorption spectrum.

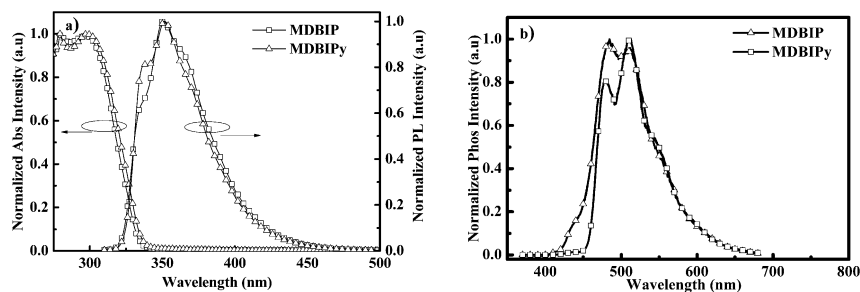


Fig. 3 (a) Room-temperature absorption (UV-Vis) and emission (PL) of **MDBIP** and **MDBIPy** in toluene solution; (b) phosphorescence (Phos) of **MDBIP** and **MDBIPy** in 2-methyltetrafuran at 77 K.

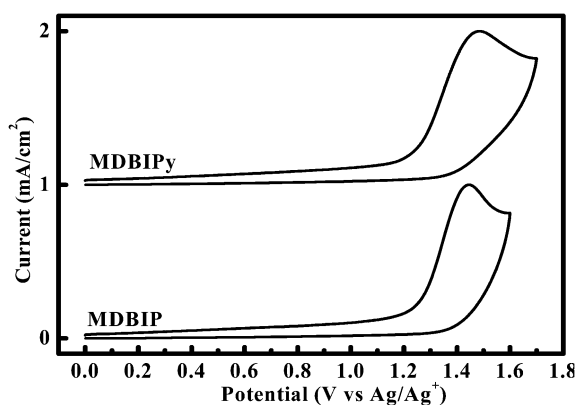


Fig. 4 The cyclic voltammetry curves of **MDBIP** and **MDBIPy**. Working electrode: Pt button; reference electrode: Ag/Ag⁺. Oxidation CV was performed in dichloromethane containing 0.1 M *n*-Bu₄NPF₆ as the supporting electrolyte at a scan rate of 100 mV s⁻¹.

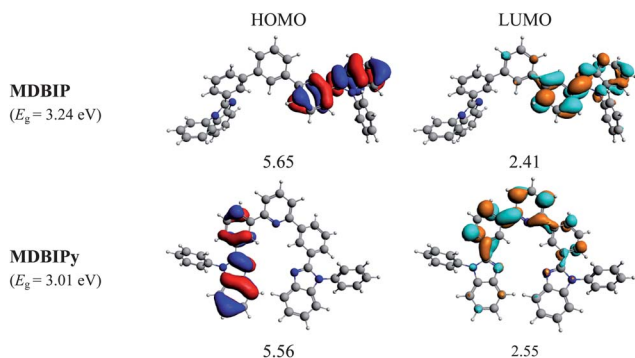


Fig. 5 Frontier molecular orbitals HOMO (left) and LUMO (right) of **MDBIP** and **MDBIPy**, calculated with DFT on a B3LYP/6-31 G(d) level.

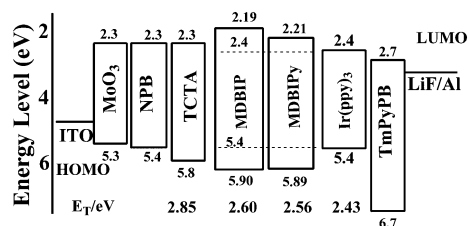


Fig. 6 Energy level diagram of the phosphorescent dyes and the device structures.

HOMO/LUMO levels (see Fig. 5) and better ET properties of **MDBIPy**, and the efficient electron injection from TmPyPB to the emissive layer can be ascribed to tunneling effects.

In order to further evaluate the electron transport character of **MDBIP** and **MDBIPy**, and the reasons that the device based on **MDBIPy** exhibits better performance, the electron mobility of the **MDBIP** and **MDBIPy** were investigated by the time-of-flight (TOF) transient-photocurrent technique. The TOF device was fabricated with the structure of ITO/Organic (2.4 μm)/Al (100 nm). The samples were illuminated at 355 nm through the ITO electrode from an optical parametric oscillator (OPO) pumped by a Q-switched Nd:YAG laser. The transient current was measured using a digital storage oscilloscope (DPO7104; bandwidth: 1 GHz). The electron mobility (μ) was calculated from the values of the transit time (T_t), the sample thickness (D) and the applied voltage (V) by using the following equation:²³

$$\mu = D^2/(VT_t)$$

As shown in Fig. 8, the material **MDBIPy** showed a relatively higher electron mobility in different electric field intensities compared to **MDBIP**. **MDBIPy** exhibits a high electron mobility about $1.5 \times 10^{-4} \text{ cm}^2 \text{ V}^{-1} \text{ s}^{-1}$ at an electric field of $8.3 \times 10^5 \text{ V cm}^{-1}$, which is comparable and even higher than those of typical electron transport materials, such as Alq₃²⁴ and OXD-7.²⁵ The relatively high electron mobility of **MDBIPy** can be ascribed to the introduction of the pyridine moiety to the molecule. As we know, pyridine is an electron-deficient moiety, which will be beneficial for accepting electrons from the anode.²⁶ All the results from the electron mobility could explain why device B has excellent performances compared to device A and imply that **MDBIPy** has the potential to be used as the ETL in PhOLEDs.

Considering the excellent electron transport ability of **MDBIPy**, we further fabricated a unilateral homogeneous device by using **MDBIPy** acting as the ETL and the host, simultaneously. The device configuration is as follows: ITO/MoO₃ (10 nm)/NPB (80 nm)/TCTA (5 nm)/**MDBIPy**: Ir(ppy)₃ (9 wt%, 20 nm)/**MDBIPy** (40 nm)/LiF (1 nm)/Al (100 nm) (device C). The J - V - B characteristics and the efficiency curves of device C are also plotted in Fig. 7(a) and (b), respectively. It was found that the drive voltages of device C are slightly higher than device B with TmPyPB as the ETL. Device C exhibits a maximum EQE of 20.6%, a maximum current efficiency of 74.2 cd A⁻¹ and a power efficiency of 71.8 lm W⁻¹, which are almost the same as those of

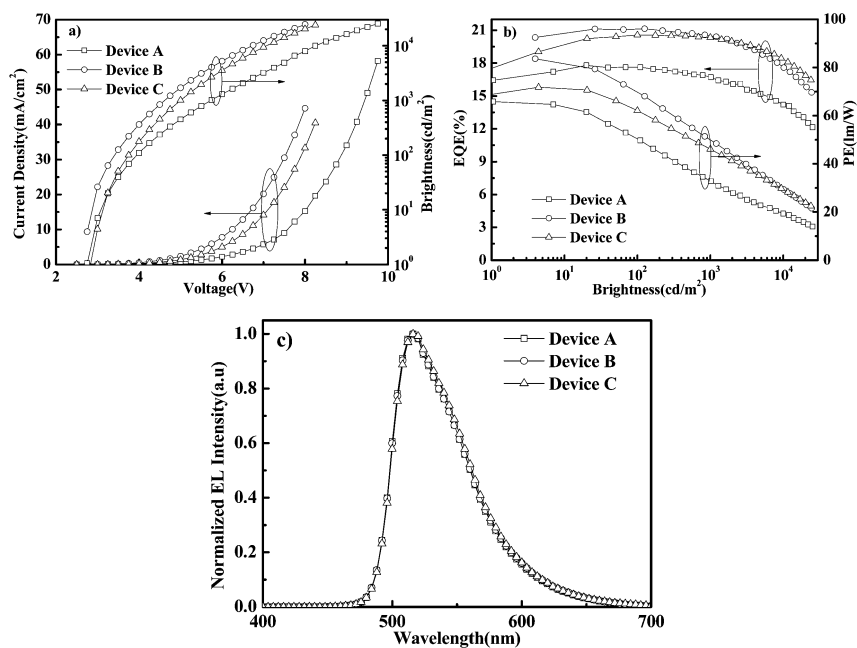


Fig. 7 (a) The current density (J)–voltage (V)–brightness (B) characteristics curves of devices A–C. (b) The external quantum efficiency (EQE) and luminous efficiency curves of the devices A–C. (c) The EL spectra for devices A, B and C at the brightness of 100 cd m^{-2} .

device B. Interestingly, device C showed low efficiency roll-off relative to device B. Such as, when the brightness of device C reaches 1000 cd m^{-2} , the EQE of the device still remains at up to 20.3%, which is even higher than device B. At a much higher brightness of 5000 cd m^{-2} , the device C still exhibited an efficiency as high as 19.4% and 69.7 cd A^{-1} . The efficiency roll-off of device C at 1000 and 5000 cd m^{-2} is only 1.1% and 5.6%, respectively, but the efficiency roll off of device B reached 2.7% and 11.2% at the same brightness. When **MDBIPy** was used as the host layer and ETL layer, simultaneously, the interface energy barrier was facilitated and the exciton recombination region was broadened, which will reduce the exciton–exciton and exciton–dipolar annihilation, and lower the roll-off of device C at high brightness. As shown in Fig. 7(c), it can be found that the EL spectra of the three devices exhibit a typical green emission from $\text{Ir}(\text{ppy})_3$, with Commission International de l’Eclairage (CIE) coordinates at around (0.29, 0.64), which indicates the complete energy transfer from host to phosphor $\text{Ir}(\text{ppy})_3$. The detailed device characteristics are shown in Table 2. Above all, these results demonstrate that utilizing an electron-type host material to fabricate unilateral homogeneous PhOLEDs is an efficient way to simplify the device structure and optimize the performance of devices.

Table 2 The electroluminescence properties of the devices^a

Device	Host/ETL	V_{on} (V)	η_c^b (cd A ⁻¹)	η_p^b (lm W ⁻¹)	EQE ^b	CIE (x, y) ^c
A	MDBIP /TmPyPB	2.8	63.7, 60.0, 54.3	65.8, 32.7, 22.3	17.8, 16.7, 15.2	(0.28, 0.64)
B	MDBIPy /TmPyPB	2.7	75.8, 73.3, 67.8	83.6, 49.8, 36.2	21.1, 20.5, 18.6	(0.29, 0.64)
C	MDBIPy / MDBIPy	2.8	74.2, 73.5, 69.7	71.8, 46.1, 34.8	20.6, 20.3, 19.3	(0.29, 0.64)

^a V_{on} : turn-on voltage; η_c : current efficiency; η_p : power efficiency; CIE (x, y): Commission International de l’Eclairage coordinates. ^b Order of measured value: maximum, values at 1000 and 5000 cd m^{-2} . ^c Measured at 100 cd m^{-2} .

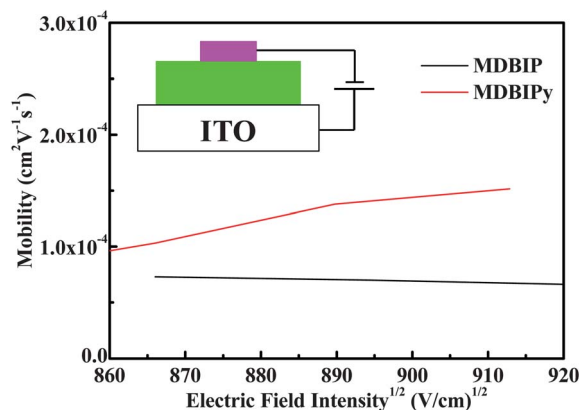


Fig. 8 The electron mobility of **MDBIP** and **MDBIPy** films plotted as a function of the square root of the electric field.

4. Conclusion

In summary, two new electron-transporting type host materials, **MDBIP** and **MDBIPy**, based on benzimidazole have been synthesized and characterized. **MDBIP** and **MDBIPy** exhibit a high decomposition temperature ($T_d = 444$ and $450 \text{ }^\circ\text{C}$) and a

good stability of surface morphology. In addition, by employing **MDBIPy** as the host for the green phosphor Ir(ppy)₃, and TmPyPB as the ETL, the PhOLEDs demonstrate excellent performance, with a maximum efficiency of 21.1%, 75.8 cd A⁻¹ and 83.6 lm W⁻¹. More interestingly, when **MDBIPy** was used as both the ETL and host material, device C showed a maximum EQE, current efficiency and power efficiency of 20.6%, 74.2 cd A⁻¹ and 71.8 lm W⁻¹, respectively. In particular, the current efficiency of device C at brightnesses of 1000 and 5000 cd m⁻² roll-offs are only 1.1% and 5.6%, respectively. Our results clearly demonstrate that utilizing an appropriate ET type host material to construct simple and high performance PhOLEDs is possible.

Acknowledgements

This research work was supported by the central allocation grant from NSFC/China (21161160442, 51203056) and Wuhan Science and Technology Bureau (no. 01010621227) and the Analytical and Testing Centre at Huazhong University of Science and Technology.

References

- (a) H.-L. Huang, Y.-J. Su, C.-L. Li, C.-H. Chien, Y.-T. Tao, P.-T. Chou, S. Datta and R.-S. Liu, *Adv. Mater.*, 2003, **15**, 884; (b) C. L. Yang, X. W. Zhang, H. You, L. Y. Zhu, L. Q. Chen, L. N. Zhu, Y. T. Tao, D. G. Ma, Z. G. Shuai and J. G. Qin, *Adv. Funct. Mater.*, 2007, **17**, 651; (c) G. Zhou, W. Y. Wong, B. Yao, Z. Xie and L. Wang, *Angew. Chem., Int. Ed.*, 2007, **46**, 1149; (d) M. A. Baldo, S. Lamansky, P. E. Burrows, M. E. Thompson and S. R. Forrest, *Appl. Phys. Lett.*, 1999, **75**, 4; (e) C. Adachi, M. A. Baldo, M. E. Thompson and S. R. Forrest, *J. Appl. Phys.*, 2001, **90**, 5048; (f) D. F. O. Brien, M. A. Baldo, Y. You, A. Shoustikov, S. Sibley, M. E. Thompson and S. R. Forrest, *Nature*, 1998, **395**, 151.
- P. E. Burrows, Z. Shen, V. Bulović, M. E. Thompson and S. R. Forrest, *Science*, 1997, **276**, 2009.
- (a) A. Chaskar, H. F. Chen and K. T. Wong, *Adv. Mater.*, 2011, **23**, 3876; (b) Y. Wei, C.-T. Chen, J.-S. Lin, M. V. R. K. Moturu, W.-S. Chao, C.-H. Chien and Y.-T. Tao, *J. Am. Chem. Soc.*, 2006, **128**, 10992.
- C. Adachi, M. A. Baldo and S. R. Forrest, *Phys. Rev. B: Condens. Matter*, 2000, **62**, 967.
- (a) Y.-M. Chen, K.-T. Wong, Y.-T. Lin, H.-C. Su and C.-c. Wu, *Org. Lett.*, 2005, **7**, 5361; (b) H.-Y. Oh, C. Kulshreshtha, J. H. Kwon and S. Lee, *Org. Electron.*, 2010, **11**, 1624; (c) F.-M. Hsu, C.-H. Chien, Y.-J. Hsieh, C.-H. Wu, C.-F. Shu, S.-W. Liu and C.-T. Chen, *J. Mater. Chem.*, 2009, **19**, 8002; (d) X. Cai, A. B. Padmaperuma, L. S. Sapochak, P. Vecchi and P. E. Burrows, *Appl. Phys. Lett.*, 2008, **92**, 083308; (e) W.-Y. Wong, C.-L. Ho, Z.-Q. Gao, B.-X. Mi, C.-H. Chen, K.-W. Cheah and Z. Lin, *Angew. Chem.*, 2006, **118**, 7964; (f) S. Gong, Y. Chen, C. Yang, C. Zhong, J. Qin and D. Ma, *Adv. Mater.*, 2010, **22**, 5370.
- H. H. Chou and C. H. Cheng, *Adv. Mater.*, 2010, **22**, 2468.
- (a) S.-J. Su, C. Cai and J. Kido, *Chem. Mater.*, 2011, **23**, 274; (b) H. Sasabe, S.-J. Su, T. Takeda and J. Kido, *Chem. Mater.*, 2008, **20**, 1691.
- Y. Tao, Q. Wang, C. Yang, Z. Zhang, T. Zou, J. Qin and D. Ma, *Angew. Chem., Int. Ed.*, 2008, **47**, 8104.
- (a) J. C. Jeong, H. S. Kim and J. G. Jang, *Mol. Cryst. Liq. Cryst.*, 2010, **530**, 103; (b) A. Takahashi, A. Endo and C. Adachi, *Jpn. J. Appl. Phys.*, 2006, **45**, 9228.
- T.-L. Chiu, P.-Y. Lee, J.-H. Lee, C.-H. Hsiao and M.-K. Leung, *J. Appl. Phys.*, 2012, **109**, 084520.
- S. O. Jeon and J. Y. Lee, *Mater. Chem. Phys.*, 2011, **127**, 300.
- M.-K. Leung, C.-C. Yang, J.-H. Lee, H.-H. Tsai, C.-F. Lin, C.-Y. Huang, Y.-O. Su and C.-F. Chiu, *Org. Lett.*, 2007, **9**, 235.
- H.-F. Chen, S.-J. Yang, Z.-H. Tsai, W.-Y. Hung, T.-C. Wang and K.-T. Wong, *J. Mater. Chem.*, 2009, **19**, 8112.
- V. A. Montes, S.-Y. Takizawa and P. Anzenbacher, Jr, *Chem. Mater.*, 2009, **21**, 2452.
- (a) C. Lee, W. Yang and R. G. Parr, *Phys. Rev. B*, 1988, **37**, 785; (b) P. A. Serena, J. M. Soler and N. Garcia, *Phys. Rev. B*, 1988, **37**, 8701.
- A. D. Boese and N. C. Handy, *J. Phys. Chem. A*, 2002, **116**, 9559.
- Z. Ge, T. Hayakawa, S. Ando, M. Ueda, T. Akiike, H. Miyamoto, T. Kajita and M.-a. Kakimoto, *Adv. Funct. Mater.*, 2008, **18**, 584.
- M. H. Tsai, Y. H. Hong, C. H. Chang, H. C. Su, C. C. Wu, A. Matoliukstyte, J. Simokaitiene, S. Grigalevicius, J. V. Grazulevicius and C. P. Hsu, *Adv. Mater.*, 2007, **19**, 862.
- Y. Z. Shaolong Gong, C. Yang, C. Zhong, J. Qin and D. Ma, *J. Phys. Chem. C*, 2010, **114**, 5193.
- H.-i. Baek and C. Lee, *J. Appl. Phys.*, 2008, **103**, 054510.
- T. Hayakawa, Z. Ge, S. Ando, M. Ueda, T. Akiike, H. Miyamoto, T. Kajita and M.-a. Kakimoto, *Org. Lett.*, 2008, **10**, 421.
- Q. Wang, J. Ding, D. Ma, Y. Cheng and L. Wang, *Appl. Phys. Lett.*, 2009, **94**, 103503.
- Y. Sun, L. Duan, D. Zhang, J. Qiao, G. Dong, L. Wang and Y. Qiu, *Adv. Funct. Mater.*, 2011, **21**, 1881.
- R. G. Kepler, P. M. Beeson, S. J. Jacobs, R. A. Anderson, M. B. Sinclair, V. S. Valencia and P. A. Cahill, *Appl. Phys. Lett.*, 1995, **66**, 3618.
- T. Yasuda, Y. Yamaguchi, D.-C. Zou and T. Tsutsui, *Jpn. J. Appl. Phys.*, 2002, **41**, 5626.
- S.-J. Su, T. Chiba, T. Takeda and J. Kido, *Adv. Mater.*, 2008, **20**, 2125.